

# Signal Demodulation of bSSFP Imaging with a Two-Point Algebraically Weighted Solution

Michael Nicholas Hoff<sup>1</sup>, and Qing-San Xiang<sup>1,2</sup>

<sup>1</sup>Physics, University of British Columbia, Vancouver, British Columbia, Canada, <sup>2</sup>Radiology, University of British Columbia, Vancouver, British Columbia, Canada

**Introduction** Balanced Steady State Free Precession (bSSFP) MRI is hindered by its sensitivity to off-resonance effects such as field inhomogeneity. While bSSFP is able to refocus substantial off-resonant magnetization, signal modulation develops from subsequent interpulse phase accumulation  $\theta$ , and dark image bands appear if  $\theta$  exceeds  $\pm 1/2TR$ . Historically, band reduction is achieved through a combination of phase cycled images with relatively shifted bands [1,2]; we recently showed that full signal demodulation and debanding is possible with four images [3,4].

While four bSSFP images require brief scan time, real time and motion-sensitive imaging would benefit from bSSFP demodulation using less data. The inherent redundancy revealed by the existence of two independent demodulation solutions [4] has inspired a new two-image approach. Here a  $\theta$ -independent algebraic solution (AS) is derived from reformulated bSSFP magnetization formulae [5] of two bSSFP images phase cycled by  $\Delta\theta = 0^\circ$  &  $180^\circ$ . A second pass Algebraically Weighted Solution (AWS) is then computed, yielding a fast technique suitable for bSSFP signal demodulation.

**Theory** Two real  $x_{1/2}$  and two imaginary  $y_{1/2}$  equations representing bSSFP signal with  $\Delta\theta_{1/2} = 0^\circ/180^\circ$  are given in Eq.1. Parameters  $M$ ,  $E_2$ , and  $b$  may be expressed in terms of flip angle  $\alpha$ , base magnetization  $M_0$ ,  $T1$  ( $E_1 = e^{-TR/T1}$ ) and  $T2$  ( $E_2 = e^{-TR/T2}$ ). The AS is found by solving for the  $\theta$ -independent magnetization parameter  $M$  in terms of the four x/y equations. Eq.2 shows the four AS solutions, where only one solution is correct for a given pixel.

$$x_{1/2} = \frac{M(1 \mp E_2) \cos \frac{\theta}{2}}{1 \mp b \cos \theta} \quad M = \frac{M_0(1 - E_1) \sin \alpha}{1 - E_1 \cos \alpha - E_2^2(E_1 - \cos \alpha)} \quad (1)$$

$$y_{1/2} = \frac{M(1 \pm E_2) \sin \frac{\theta}{2}}{1 \mp b \cos \theta} \quad b = \frac{E_2(1 - E_1)(1 + \cos \alpha)}{1 - E_1 \cos \alpha - E_2^2(E_1 - \cos \alpha)}$$

$$M_1 = \frac{\sqrt{x_1 x_2 + y_1 y_2} (x_2 y_1 + \sqrt{x_1 x_2 y_1 y_2})}{\pm (y_1 \sqrt{x_1 x_2} + x_2 \sqrt{y_1 y_2})} \quad (2)$$

$$M_3 = \frac{\sqrt{x_1 x_2 + y_1 y_2} (x_2 y_1 - \sqrt{x_1 x_2 y_1 y_2})}{\pm (y_1 \sqrt{x_1 x_2} - x_2 \sqrt{y_1 y_2})}$$

$$\text{Error} \quad \sigma_i = 1000 \frac{\sqrt{\sum_{x,y} [M_i(x,y) - M_g(x,y)]^2}}{\sum_{x,y} M_g(x,y)} \quad (3)$$

**Methods** The solution was applied to two simulated and two MR phantom images with  $\Delta\theta_{1/2} = 0^\circ/180^\circ$ ,  $\alpha = 40^\circ$ , and  $TE/TR = 2.1/4.2ms$ . Simulations employed Eq.1 with  $\theta = -2\pi \rightarrow 2\pi$  varied horizontally,  $T1/T2 = 420/50$ ,  $240/70$ , and  $2400/1400$  stacked vertically (top to bottom), and added Gaussian noise (Fig.1A).  $60 \times 3mm$  slices of 3D TrueFISP/bSSFP phantom data were acquired using a 1.5T Siemens Avanto scanner imaging a water bottle holding a Lego<sup>TM</sup> structure and a Zimmer<sup>TM</sup> (Warsaw, IN) Co-Cr-Mo alloy hip prosthesis to provide field inhomogeneity (Fig.2A). Phase was corrected for spatial drift and offset. Data was processed pixel-by-pixel: image real parts  $x_{1/2}$  and imaginary parts  $y_{1/2}$  were input into the four AS equations (Eq.2), and solutions were sifted for feasibility. A golden section numerical minimization of the regional least squares residual between a weighted solution of the original data and the sifted AS yielded the AWS. Total relative error  $\sigma$  (Eq.3) was calculated for the AWS and a two-image complex sum (CS) with respect to a gold standard  $M_g$ , which is the known magnetization for the simulated data, and the geometric cross-solution (XS, [3]) for the phantom.

**Results** Fig.1 depicts one of the two simulated images ( $\Delta\theta = 0^\circ$ ), the AS, sifted AS, AWS, and CS. The CS has residual bands in all three regions, while the AWS only has bands in the bottom region. Fig. 2 shows one bSSFP phantom image ( $\Delta\theta = 0^\circ$ ), the AS, AWS, and CS. The AWS shows considerable band reduction relative to the CS. The red  $\sigma$  values indicate that the AWS has consistently less deviation from the gold standard than the CS for both real and simulated data.

**Discussion** A two image solution to the bSSFP banding problem is formulated and its performance is compared to the complex sum. Phase correction and simple sifting of the four-part solution are necessary for predictable  $\theta$ -demodulation. Brief post-processing via a regional numerical optimization routine is employed to mitigate residual instabilities at the band centres. The AWS outperforms the CS, and employs only two images, demonstrating its value for signal demodulation in time-constrained bSSFP imaging.

**References** [1] Zur *et al.*, MRM, 16:444-459, 1990. [4] Hoff & Xiang, Proc. ISMRM, 19: 2824, 2011.

[2] Bangertner *et al.*, MRM, 51:1038-1047, 2004. [5] Ernst & Anderson, Rev Sci Instrum, 37:93-102, 1966.

[3] Xiang & Hoff, Proc. ISMRM, 18:74, 2010.

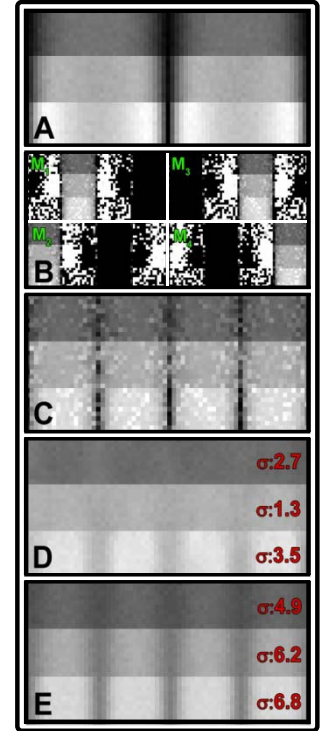


Fig.1: bSSFP noisy simulated images. A. 1 of 2 original images. B. Algebraic Solution (AS),  $M_1 \rightarrow M_4$  (Eq.2). C. Sifted AS. D. Algebraically Weighted Solution. E. Complex Sum.

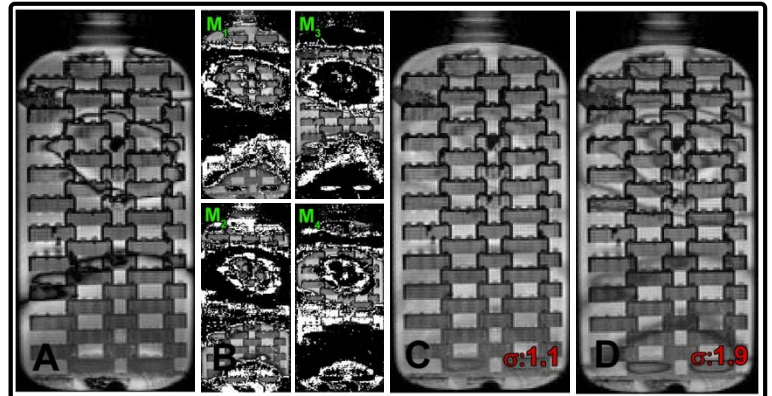


Fig.2: MR Phantom Images. A. 1 of 2 original images. B. Algebraic Solution,  $M_1 \rightarrow M_4$  (Eq.2). C. Algebraically Weighted Solution. D. Complex Sum.